Computational Materials Science 81 (2014) 141–145

Contents lists available at ScienceDirect

Computational Materials Science

journal homepage: www.elsevier.com/locate/commatsci

Magneto-electronic studies of anti-perovskites $NiNMn_3$ and $ZnNMn_3$

Zahid Ali [a], M. Shafiq [a], S. Jalali Asadabadi [b], H.A. Rahnamaye Aliabad [c], Imad Khan [a], Iftikhar Ahmad [a,*]

[a] Center for Materials Modeling and Simulations, University of Malakand, Chakdara, Pakistan
[b] Department of Physics, Faculty of Science, University of Isfahan, Hezar Gerib Avenue, Isfahan 81744, Iran
[c] Department of Physics, Hakim Sabzevary University, Sabzevar, Iran

ARTICLE INFO

Article history:
Received 29 January 2013
Received in revised form 19 July 2013
Accepted 28 July 2013
Available online 12 September 2013

Keywords:
Anti-perovskites
Electronic band structure
DFT
Anti-ferromagnetism

ABSTRACT

Density functional theory is used to investigate the structural, electronic and magnetic properties of the anti-perovskites $NiNMn_3$ and $ZnNMn_3$. The calculated structural parameters are found consistent with the experimental results. The spin-polarized calculations of the electronic properties show metallic nature of these compounds. Furthermore the magnetic phase for each compound is optimized, which reveals that both of these compounds prefer anti-ferromagnetic phase. The calculated effective magnetic moments are also found consistent with the experimental values. The studies presented in this paper confirm the magnetoresistive nature of these compounds.

1. Introduction

The unique physical properties of the anti-perovskite compounds are very attractive for advance hybrid devices [1]. The anti-perovskite compounds have gained considerable attention because of their interesting physical properties derived from the relationship between magnetic properties and crystal lattice, such as magnetostriction [2], giant magnetoresistance (GMR) [3,4], low temperature coefficient resistivity (L-TCR) [1], negative thermal expansion (NTE) [5] and superconductivity at high temperature [6,7].

Mn-based anti-perovskite $XAMn_3$ series with X = Ga, Zn, Cu, Ge, Sn, Ni and A = N, C, B are metallic compounds with cubic structure and space group Pm-3m. In these compounds A-atom lies at the body-centered, Mn atoms are located on the face-centered, and X-atom occupies the corners of a unit cell [8]. A comparison of perovskite and anti-perovskite show that transition metal has six nearest neighbor oxygens in perovskite structure, while Mn atom has only two nearest neighbors (A-atoms) in the anti-perovskite structure [9]. In anti-perovskite compounds the oxygen atoms are replaced by transition metals (TM). In $XAMn_3$, when cation-X and anion-A sites are replaced by different elements (X = Ga, Zn, Cu, Ge, Sn, Ni and A = N, C, B), an extended family of Mn-based anti-perovskites can be obtained [10]. Due to strong hybridization near Fermi level $ANMn_3$ (A = Ni, Zn, Sn, etc.) narrow bands are formed which depends on the number of valence electrons on A site, because A site atom makes the system itinerant at Fermi level [11]. These compounds show paramagnetic (PM) behaviour at high temperature and anti-ferromagnetic (AFM) or ferromagnetic (FM) at low temperatures [2,12].

The manganese nitride anti-perovskites have a number of advantages over other materials, where they are stable in air and mechanically hard as well as formed of economically cheaper materials such as Mn, Ni and Zn. Manganese nitrides are also metallic and have high electric and thermal conductivity [13].

Cubic anti-perovskite materials $ANMn_3$ (A = Ni and Zn) are similar to perovskite oxides [14]. Chu et al. [11] and Kim et al. [15] experimentally prepared the polycrystalline sample of $ANMn_3$ by mixing powder of Mn_2N and pure A (A = Ni and Zn) in a bag filled with nitrogen gas potted in an evacuated quartz tube. They determined the cubic structure of the compound with a space group Pm-3m by the Rietveld refinement method using powder neutron diffraction data.

Between 160 K and 266 K temperature the magnetic structure of $NiNMn_3$ is the combination of two triangular AFM structures Γ^{4g} and Γ^{5g} while below 160 K it exists in Γ^{5g} AFM structure [12,16] $ZnNMn_3$ show different magnetic structures and properties than $NiNMn_3$. It changes from paramagnetic (PM) phase to AFM phase at lower temperature with triangular Γ^{5g} structure [17]. These compounds does not favor ferromagnetic phase; however similar to $NiNMn_3$ a direct transition from AFM to PM occurs with the increase in temperature [8,9]. The magnetic phase transition from AFM to PM in $ZnNMn_3$ occurs at 190 K [18] $ZnNMn_3$ sometimes shows sudden and irregular increase of few percent in lattice volume at transition temperature from PM to AFM, which is called magneto-volume effect (MVE) [5,19]. The magnetic transitions are isostructural so that the crystal structure remains the same.

* Corresponding author. Tel.: +92 332 906 7866.
E-mail addresses: dr.iftikhar@uom.edu.pk, ahma5532@gmail.com (I. Ahmad).

0927-0256/$ - see front matter © 2013 Elsevier B.V. All rights reserved.
http://dx.doi.org/10.1016/j.commatsci.2013.07.040

Table 1
Calculated lattice constant (a_o), bulk modulus (B), derivative of bulk modulus (B'), ground state energy in ferromagnetic (E_{FM}) and anti-ferromagnetic (E_{AFM}) phases, energy difference between FM and AFM phases ($\Delta E_{FM\text{-}AFM}$), and bond length (d) in the cubic anti-perovskites $NiNMn_3$ and $ZnNMn_3$ compounds.

Parameters	$NiNMn_3$	$ZnNMn_3$
a_o (Å)	3.7875	3.7802
Exp.	3.886[a]	3.884[b]
B (GPa)	133.6735	260.2162
B'	1.9043	8.1929
E_{FM} (Ry)	−10093.5868	−10643.9448
E_{AFM} (Ry)	−10093.5930	−10643.9980
$\Delta E_{FM\text{-}AFM}$ (Ry)	0.0062	0.0532
d_{Mn-N} (Å)	1.8637	1.8602
$d_{Mn-Ni/Zn}$ (Å)	2.6357	2.6306

[a] [16].
[b] [15].

Therefore the magneto-volume effect is isotropic [13]. The partial substitution of metal (e.g., Ag, Ge and Ga), in anti-perovskite manganese nitrides $XNMn_3$ on Ni and Zn sites make them suitable materials for large negative thermal expansion (NTE) effects and zero thermal expansion (ZTE) which can be used in optical applications magnetostriction, engineering and electronics [5,11,20,21]. Those materials which contract on heating show negative thermal effects have many practical applications [22]. In these compounds NTE occurs due to MVE [23]. The NTE materials are needed to control thermal expansion of materials, which have been widely used for technical applications in high-precision (zero-expansion) optical and machinery parts, printed circuit boards and heat sinks and an athermalizer for a Bragg gratings [24,25].

In present work we have theoretically studied the structural, electronic and magnetic properties of Mn-based anti-perovskites $NiNMn_3$ and $ZnNMn_3$ using generalized gradient approximation

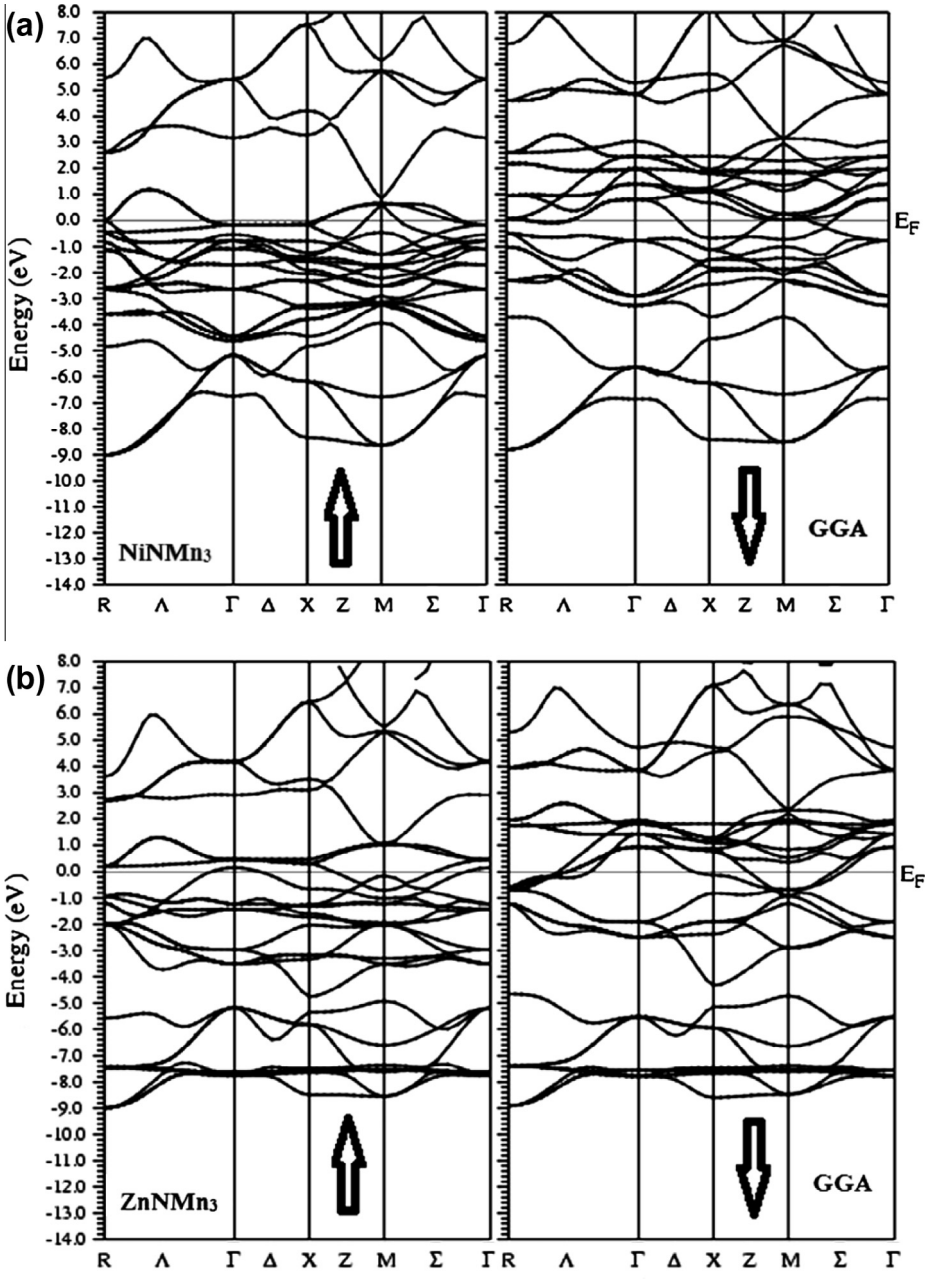

Fig. 1. Spin-dependent electronic band structure by GGA (a) $NiNMn_3$ and (b) $ZnNMn_3$.

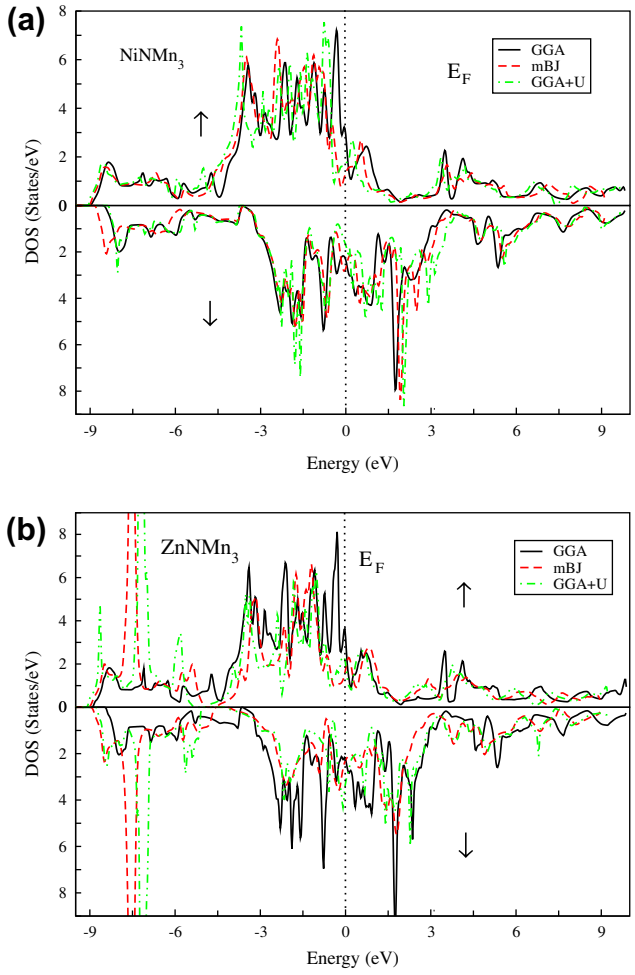

Fig. 2. Spin-dependent total DOSs of (a) $NiNMn_3$ and (b) $ZnNMn_3$ per unit cell by GGA, mBJ and by GGA + U.

(GGA), modified Becke–Johnson (mBJ) and GGA + U within the framework of density functional theory (DFT). The aim of the present work is to explore the physical properties of these compounds for their possible technological applications and also provide theoretical basis to the available experimental results. The electronic structures of both of the compounds are investigated on the basis of the electronic band structures, total and partial densities of states. The stable magnetic phases of these compounds are evaluated by comparing the total energies in ferromagnetic (FM) and AFM states. In order to obtain better magnetic properties of these compounds an optimized effective Hubbard parameter U is also used.

2. Computational details

In the present work the Kohn–Sham equations [26] are solved to calculate the structural, electronic and magnetic properties of the cubic anti-perovskite $ANMn_3$ (A = Ni and Zn). The full potential linearized augmented plane waves (FP-LAPW) method [27] with GGA [28], GGA + U [29–32] and mBJ potential [33,34] are used to solve Kohn–Sham equations. mBJ is an exchange potential and is used in combination with GGA to handle exchange and correlation energy for strongly correlated electron systems [35,36]. Details of the FP-LAPW method, formulas and the wien2k software used in the present calculations can be found in Ref. [37].

The core electrons are treated fully relativistically and the valence electrons are treated semi-relativistically. In order to ensure

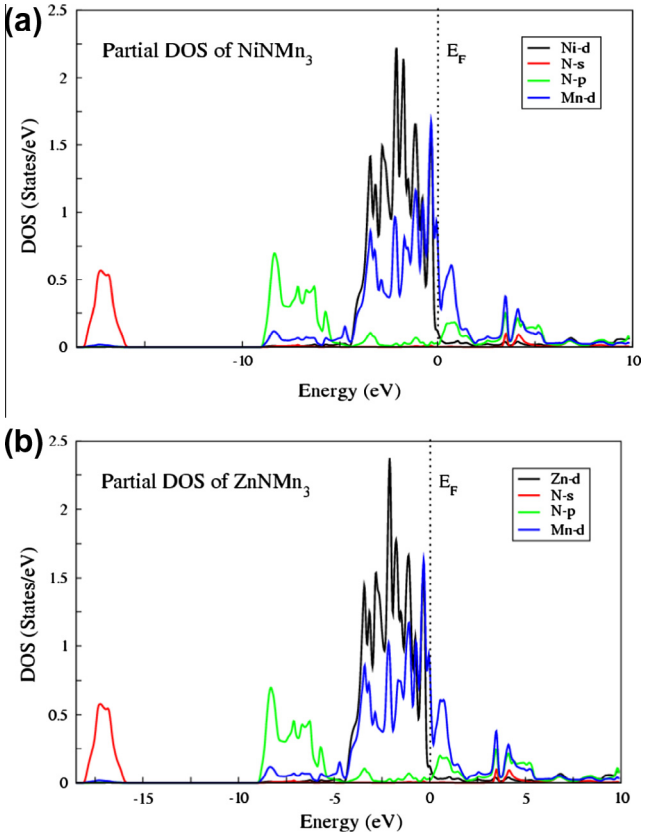

Fig. 3. Partial DOSs of (a) $NiNMn_3$ and (b) $ZnNMn_3$.

that no electron leakage is taking place semi-core states are included and are described with local orbitals. To ascertain that the results are accurately converged, an approximated correction value is chosen for $U_{eff} = U–J$ after examining and testing several values of Hubbard potential in order to adjust the Mn-3d orbitals level in the density of states. In order to get better magnetic properties the U_{eff} is eventually optimized to 0.07 Ry. For all calculations 286 k-points and $R_{MT} \times K_{max} = 8.00$ basis functions are used.

3. Results and discussion

3.1. Structural properties

For the structural properties of $NiNMn_3$ and $ZnNMn_3$ the total energies of the crystals are minimized with respect to the unit cell volumes using the Birch–Murnaghan equation of state [38] in analogy to our previous works [39–41]. The calculated structural parameters such as lattice constants, bulk moduli, derivative of bulk moduli and ground state energies corresponding to the optimum volumes are shown in Table 1. It is obvious from the table that our calculated lattice parameter for $NiNMn_3$ is 2.53% and $ZnNMn_3$ is 2.67% less than their experimental values [15,16]. Our results, as presented in Table 1, show that the lattice parameter of $NiNMn_3$ is smaller than $ZnNMn_3$. This shows that the lattice constants of the compounds under investigation, i.e., $ANMn_3$, are predicted to be contracted as the atomic number of the A increases (A = Ni and Zn). The contraction of the lattice parameter may be attributed to the regular d-block contraction of the atomic radius as we go along the d-block period of the periodic table from left to right. The bonds length between different atoms of these compounds are also calculated and presented in Table 1. The difference in Mn–N bond lengths, $d_{Mn\text{-}N}$, in $NiNMn_3$ and $ZnNMn_3$ compounds

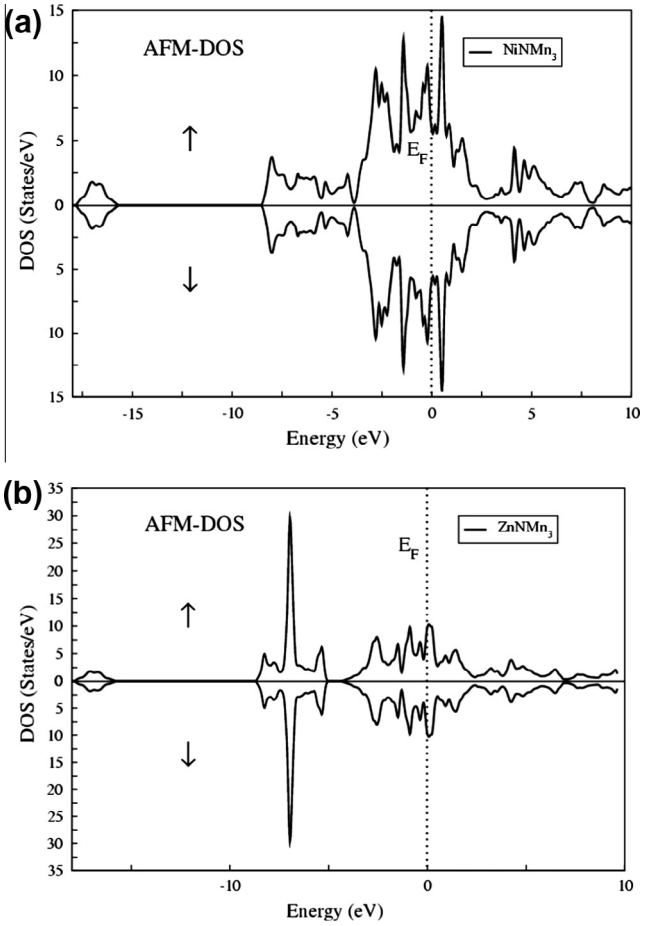

Fig. 4. AFM DOS for the double cell of (a) $NiNMn_3$ and (b) $ZnNMn_3$.

reveals that in our calculations Mn–N spacing in $ZnNMn_3$ is smaller than that of $NiNMn_3$ most likely due to its smaller lattice constant compared to the other compound.

3.2. Electronic band structures and densities of states

Self-consistent calculations are performed in order to explore the electronic nature of the cubic $NiNMn_3$ and $ZnNMn_3$ compounds. Spin-dependent electronic band structures of both the compounds are presented in Fig. 1(a and b). It is clear from the figures that by GGA, the majority spin (↑) and minority spin (↓) states cross the Fermi level and overlap the conduction bands. Hence, these compounds show metallic nature. Our results are in agreement with the results of Refs. [13,42].

The origin of band structures of the can be understood by the total density of states. The total DOSs for both of the compounds are calculated by GGA, mBJ and GGA + U as shown in Fig. 2(a and b). To explain the contribution of different states in the band structures, partial densities of states are calculated for both compounds by GGA and mBJ, presented in Fig. 3(a and b). The results, as presented in Fig. 3(a), show that for $NiNMn_3$ the occupied states include semicore and valance states are distributed over an energy interval ranging from −18.1 eV to Fermi level. The semicore states are mainly occupied by N-2s. Thus, the N-2s states play comparatively minor role in the physical properties of the system. If we abandon the N-2s states towards the Fermi level, we encounter first a large gap, second mainly the N-2p states, and eventually Ni-d and Mn-d states. Thus, the valence region is predominant by the Ni-3d and Mn-3d with a small contribution arising from N-2p. In the valence band the main peak at −2.12 eV is due to Ni-3d and the peak just below the Fermi level at −0.45 eV is due to Mn-3d state. There exists strong hybridization between Ni-3d, Mn-3d and N-2p states around the Fermi level. The strong hybridization between N-2p and Mn-3d states near the Fermi level forms narrow bands. These bands changes considerably according to the number of valence electrons of Ni atom. Thus the A atom (A = Ni, Zn) makes the system as an itinerant electron system. Strong hybridization around the Fermi level makes the material metallic. Beyond the Fermi level, the unoccupied band structures are mostly originated by Mn-3d state hybridized with N-2s, N-2p and Ni-3d states.

Fig. 3(b) shows the partial density of states of $ZnNMn_3$. It is clear from Fig. 3(a and b) that the shapes of $NiNMn_3$ and $ZnNMn_3$ DOS are almost similar. One of the differences is the maximum peak of Ni-3d DOS for $NiNMn_3$ 2.25 states/eV, which is comparable to the maximum peak of Zn-3d DOS for $ZnNMn_3$ 2.38 states/ eV. The peak of Zn-3d is maximum because the 3d-state of Zn is more stable as compared to 3d-state of Ni. However the difference is almost negligible and does not significantly affect the electronic nature of these compounds.

3.3. Magnetic properties

In order to study the stability of the magnetic phases, we optimize the compounds under investigation by constructing two individual structures for setting up for anti-ferromagnetic and ferromagnetic phases. For the anti-ferromagnetic calculations the ↑↓ magnetic ordering is considered for the atoms containing 3d orbitals. The optimized values of these compounds are presented in Table 1. It is obvious from the table that both, $NiNMn_3$ and $ZnNMn_3$, systems prefer to be ordered anti-ferromagnetically as their calculated energies in the AFM phase, E_{AFM}, are lower than those in the FM phase, E_{FM}, and thereby $\Delta E_{FM\text{-}AFM} = E_{FM} - E_{AFM} > 0$. Our calculations are in agreement with the experimental results of Fruchart (1978) [12] in which AFM is the ground state for both $NiNMn_3$ and $ZnNMn_3$ crystals. The calculated DOS's for both of the AFM, $NiNMn_3$ and $ZnNMn_3$, compounds are presented in Fig. 4(a and b). It is clear from the figures that the DOS is symmetric for

Table 2
Calculated magnetic moments in unit of (μ_B) interstitial, local and total magnetic moments of $NiNMn_3$ and $ZnNMn_3$ per unit cell.

Magnetic moments	$NiNMn_3$			$ZnNMn_3$		
	GGA	mBJ	GGA + U	GGA	mBJ	GGA + U
M^T	5.8580	5.1888	6.6500	7.2979	4.5952	6.98357
M^{inst}	0.4069	0.3920	0.8079	0.3866	0.1904	0.46183
$M^{Ni/Zn}$	0.7004	0.8965	0.8980	0.8788	−0.1052	−0.1120
M^N	−0.1102	−0.1718	−0.2142	−0.1018	−0.1606	−0.1107
M^{Mn}	1.5563	1.6572	1.8203	2.0447	1.5569	2.2481
Exp			1.8[a]			2.2[b]

[a] [12].
[b] [15].

both spin states. Therefore, the total magnetic moments are calculated to be zero for both AFM cases. Hence, both of the compounds $NiNMn_3$ and $ZnNMn_3$ prefer to be AFM, because their AFM energies are less than their FM energies which is in agreement with the experiments [12,15].

Magnetism in perovskites is due to indirect exchange interaction between TM–TM via nonmagnetic anion, one is called double exchange and other is super exchange [39]. Double exchange favors ferromagnetism in most of the cases and super exchange antiferromagnetism. Zener [43] introduced the concept of immediate transfer of electron from transition metal to the oxygen and from the oxygen to the neighboring transition metal. The magnetic moments of $NiNMn_3$ and $ZnNMn_3$ per unit cell are calculated by GGA, mBJ and GGA + U. The calculated interstitial, local and total magnetic moments for all the compounds are presented in Table 2. It can be seen from Table 2 that Mn atom is mainly responsible for magnetism in these compounds. For GGA + U calculations, we used the effective value of 0.07 Ry. For anti-ferromagnetic compounds $NiNMn_3$ and $ZnNMn_3$ the magnetic moments per unit cells arises from Mn atoms are 1.82 μB and 2.24 μB respectively calculated by GGA + U. The results are in good agreement with the experiments reported in Refs. [12,15].

4. Conclusions

In summary we have theoretically studied the structural, electronic and magnetic properties of anti-perovskites $NiNMn_3$ and $ZnNMn_3$ using the all electron full potential linearized augmented plane wave method within the frame work of the density functional theory. The structural parameters are found consistent with the experimental data. The electronic properties of these compounds are evaluated on the bases of spin dependent electronic band structures and total and partial densities of states, which show that these compounds are metallic. The magnetic stable state for each compound is optimized which reveal that $NiNMn_3$ and $ZnNMn_3$ are anti-ferromagnetic. The effective magnetic moments are found in close agreement with the experimental values. On the basis of the above theoretical studies it is predicted that $NiNMn_3$ and $ZnNMn_3$ magnetoresistive materials and need extensive experimental studies for their possible applications in the advance technology.

References

[1] E.O. Chi, W.S. Kim, N.H. Hur, Solid State Commun. 120 (2001) 307.
[2] K. Asano, K. Koyama, K. Takenaka, Appl. Phys. Lett. 92 (2008) 161909.
[3] K. Kamishima, T. Goto, H. Nakagawa, N. Miura, M. Ohashi, N. Mori, T. Sasaki, T. Kanomata, Phys. Rev. B 63 (2000) 024426.
[4] Y.B. Li, W.F. Li, W.J. Feng, Y.Q. Zhang, Z.D. Zhang, Phys. Rev. B 72 (2005) 024411.
[5] K. Takenaka, Appl. Phys. Lett. 87 (2005) 261902.
[6] T. He, Q. Huang, A.P. Ramirez, Y. Wang, K.A. Regan, N. Rogado, M.A. Hayward, M.K. Haas, J.S. Slusky, K. Inumara, H.W. Zandbergen, N.P. Ong, R.J. Cava, Nature (London) 411 (2001) 54.
[7] M. Uehara, T. Yamazaki, T. Kori, T. Kashida, Y. Kimishima, I. Hase, J. Phys. Soc. Jpn. 76 (2007) 034714.
[8] X.B. Kong, Y. Sun, L.X. Yang, Y. Yu, C.Q. Jin, C. Wang, R.C. Yu, J. Appl. Phys. 106 (2009) 113905.
[9] J.H. Shim, S.K. Kwon, B.I. Min, Phys. Rev. B 66 (2002) 020406.
[10] W.J. Feng, D. Li, W.J. Ren, Y.B. Li, W.F. Li, J. Li, Y.Q. Zhang, Z.D. Zhang, J. Alloys Compd. 437 (2007) 27.
[11] L. Chu, C. Wang, J. Yan, Y. Na, L. Ding, Y. Sun, Y. Wen, Scr. Mater. 67 (2012) 173.
[12] D. Fruchart, E.F. Bertaut, J. Phys. Soc. Jpn. 44 (1978) 781.
[13] K. Takenaka, H. Takagi, Mater. Trans. 47 (2006) 471.
[14] S. Jin, T.H. Tiefel, M. McCormack, R.A. Fastnacht, R. Ramesh, L.H. Chen, Science 264 (1994) 413.
[15] W.S. Kim, E.O. Chi, J.C. Kim, N.H. Hur, K.W. Lee, Y.N. Choi, Phys. Rev. B 68 (2003) 172402.
[16] D. Fruchart, E.F. Bertaut, R. Madar, G. Lorthioir, R. Fruchart, Solid State Commun. 9 (1971) 1793.
[17] T. Hamada, K. Takenaka, J. Appl. Phys. 111 (07) (2012) A904.
[18] Y.S. Sun, Y.F. Guo, X.X. Wang, Y. Tsujimoto, Y. Matsushita, Y.G. Shi, C. Wang, A.A. Belik, K. Yamaura, Appl. Phys. Lett. 100 (2012) 161907.
[19] S. Iikubo, K. Kodama, K. Takenaka, H. Takagi, S. Shamoto, Phys. Rev. B 77 (2008) 020409.
[20] K. Takenaka, H. Takagi, Appl. Phys. Lett. 94 (2009) 131904.
[21] C. Wang, L. Chu, Q. Yao, Y. Sun, M. Wu, L. Ding, J. Yan, Y. Na, W. Tang, G. Li, Q. Huang, J.W. Lynn, Phys. Rev. B 85 (2012) 220103.
[22] A.W. Sleight, Curr. Opin. Solid State Mater. Sci. 3 (1998) 128.
[23] A.W. Sleight, Inorg. Chem. 37 (1998) 2854.
[24] A. Sakamoto, T. Matano, H. Takeuchi, IEICE Trans. Electron. E 83 (2000) 1441.
[25] K. Kintaka, J. Nishii, Y. Kawamoto, A. Sakamoto, P.G. Kazansky, Opt. Lett. 27 (2002) 1394.
[26] W. Kohn, L.S. Sham, Phys. Rev. A 140 (1965) 1133.
[27] O.K. Andersen, Phys. Rev. B 12 (1975) 3060.
[28] J.P. Perdew, A. Ruzsinszky, G.I. Csonka, O.A. Vydrov, G.E. Scuseria, L.A. Constantin, X. Zhou, K. Burke, Phys. Rev. Lett. 101 (2008) 239702.
[29] A.G. Petukhov, Phys. Rev. B 67 (2003) 153106.
[30] P. Novak, J. Kunes, L. Chaput, W.E. Pickett, Phys. Stat. Sol. B 243 (2006) 563.
[31] V.I. Anisimov, I.V. Solovyev, M.A. Korotin, M.T. Czyzyk, G.A. Sawatzky, Phys. Rev. B 48 (1993) 16929.
[32] Z. Ali, I. Ahmad, S.A. Jalali, Comput. Mater. Sci. 67 (2013) 151.
[33] A.D. Becke, E.R. Johnson, J. Chem. Phys. 124 (2006) 221101.
[34] F. Tran, P. Blaha, K. Schwarz, J. Phys. Condens. Matter. 19 (2007) 196208.
[35] I. Khan, I. Ahmad, H.A. Rahnamaye Aliabad, M. Maqbool, J. Appl. Phys. 112 (2012) 073104.
[36] I. Khan, I. Ahmad, H.A.R. Aliabad, S.J. Asadabadi, Z. Ali, M. Maqbool, Comput. Mater. Sci. 77 (2013) 145.
[37] P. Blaha, K. Schwarz, G.K.H. Madsen, D. Kvasnicka, J. Luitz, WIEN2k, An Augmented Plane Wave Plus Local Orbitals Program for Calculating Crystal Properties, Vienna University of Technology, Vienna, Austria, 2001.
[38] F. Birch, Phys. Rev. 71 (1947) 809.
[39] Z. Ali, I. Ahmad, B. Amin, M. Maqbool, G. Murtaza, I. Khan, M.J. Akhtar, F. Ghafor, Physica B 406 (2011) 3800.
[40] Z. Ali, I. Ahmad, I. Khan, B. Amin, Intermetallics 31 (2012) 287.
[41] I. Khan, A. Afaq, H.A.R. Aliabad, I. Ahmad, Comput. Mater. Sci. 61 (2012) 278.
[42] L. Ding, C. Wang, L. Chu, J. Yan, Y. Na, Q. Huang, X. Chen, Appl. Phys. Lett. 99 (2011) 251905.
[43] C. Zener, Phys. Rev. 82 (1951) 403.